

# Comparative Study of Fault Identification and Classification on EHV Lines Using Discrete Wavelet Transform and Fourier Transform Based ANN

K.Gayathri and N. Kumarappan, Senior Member, IEEE

**Abstract**—An appropriate method for fault identification and classification on extra high voltage transmission line using discrete wavelet transform is proposed in this paper. The sharp variations of the generated short circuit transient signals which are recorded at the sending end of the transmission line are adopted to identify the fault. The threshold values involve fault classification and these are done on the basis of the multiresolution analysis. A comparative study of the performance is also presented for Discrete Fourier Transform (DFT) based Artificial Neural Network (ANN) and Discrete Wavelet Transform (DWT). The results prove that the proposed method is an effective and efficient one in obtaining the accurate result within short duration of time by using Daubechies 4 and 9. Simulation of the power system is done using MATLAB.

**Keywords**—EHV transmission line, Fault identification and classification, Discrete wavelet transform, Multiresolution analysis, Artificial neural network.

## I. INTRODUCTION

IN the transmission line short circuit fault occurs due to several reasons. It might be due to lightning strike, tree branches falling on transmission line, fog and many more. This may give raise to the consequence of permanent damage to the line insulators. So it has become necessary to analyze the fault on the transmission line in a better approach. The occurrence of any transmission line fault gives raise to a transient condition. The transient phase is marked by the presence of harmonic current.

So far, several techniques are adopted for pattern recognition of generating the high frequency signals. ANN [2, 3] is used to identify and classify the faults. But the drawback of this method is the resolution is not efficient. Fourier Transform (FT) [4] is used in these schemes to process the original time domain signal but it may give raise to inaccurate spectra leading to frequency leaking and has poor time localized property for high frequency components of the signal. However, the problem of FT can be resolved by

using Short Time Fourier Transform (STFT) [5, 6], which windows the input signal. As a single window is used for all frequencies, resolution of the STFT cannot vary for different frequencies.

Many researches had been done using wavelet transform to analyze the performance of it. The wavelet transform provides a better detection when the signals changes abruptly [9], so it is praiseworthy for fault detection since the faulted signals changes abruptly. Wavelet transform is adopted to discriminate the faults type from the magnetizing inrush current [7] in the transformer and then wavelet transform is used for fault identification and classification [10]. Multiresolution capability is advanced technique of wavelet transform which makes windows automatically and identifies and classifies the faults for the different signals [11], but the threshold values implemented for fault detection is not mentioned. By considering the above mentioned method, faults are classified [12] but fault impedance and fault inception angle are not taken into consideration. The same wavelet approach is also used to classify faults in the underground cable system [1]. Moreover the wavelet transform gives result closely related to IEC (International Electro technical Commission) standard framework [14] for harmonic analysis in power system.

The proposed analysis involves the multiresolution method, where the threshold values are employed to identify and classify faults. In this approach DFT limitations are overcome by wavelet transform method which uses short windows for high frequencies and long windows for low frequencies.

## II. PROPOSED METHOD AND ITS IMPLEMENTATION

### A. Simulation Study

The simulations were done on a simple transmission line circuit consisting of a generator at one end and a load at the other end and the line is extended to 150 km without mutual coupling. The base value of the voltage in the system is 400kV. The frequency of the system is 50Hz. Simulation of the simple power system is done using MATLAB. Fig.1 [3] shows the power system under study, in which FI and FC denotes Fault Identification and Fault Classification respectively. The transmission line is represented by lumped

K.Gayathri (g.gayathri3@gmail.com) and N.Kumarappan (kumarappan\_n@yahoo.com) are with Department of Electrical Engineering, FEAT, Annamalai University, Annamalainagar – 608 002, Tamilnadu, India. (corresponding author to provide phone: +91-4144-239152; email: g.gayathri3@gmail.com).

parameters (3 Pi sections are used) and its parameters frequency dependence is taken into consideration without mutual coupling [17].

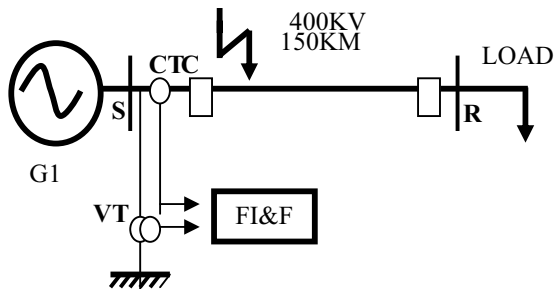


Fig. 1. Power system under study

This method is not based on the amplitude of the voltage transient but on the frequency found in the transients. This is the major advantage of this method. This method was tested with four different values of internal impedance of the generator and the load models taken for the test are, in case 1, source resistance is 0.5ohm and source inductance is 10e-3. In case 2, source resistance is 0.89 ohm and source inductance is 16.58e-3. In case 3, source resistance is 1 ohm and source inductance is 30e-3. In case 4, source resistance is 2 ohm and source inductance is 60e-3 with fault points (distance of the fault) taken for test were 10, 20, 30, 40, 50, .....120km. The different values of fault resistance were 5, 10, 20 ohms.

Fig. 2 shows the proposed method's functional block diagram. The voltage and current waveforms of the simulated power system are fed as input to the sampling network. The signals are sampled at 50 KHz [5] to obtain higher resolution. The sampled signals are given to the discrete wavelet transform to identify and classify the faults. Thus different types of faults are classified. The proposed method is also applicable to a double-circuit untransposed line.

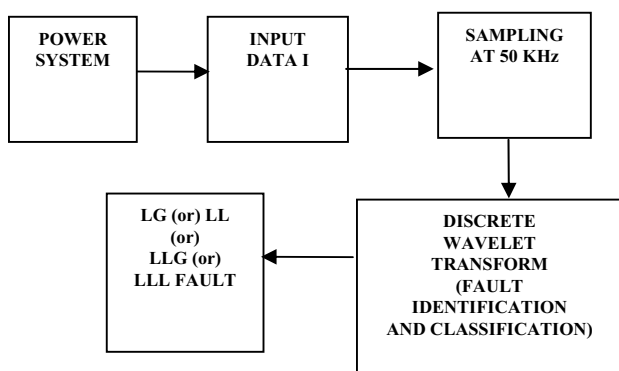


Fig. 2. Function block diagram of DWT method

### B. Wavelet Transform

A wavelet is an oscillatory waveform of effectively limited duration that has an average value of zero, waving above and below x-axis. In particular, the wavelet transform is of interest for the analysis of non-stationary signals which does not change periodically with time. Wavelet are functions that satisfy the requirements of both time and frequency localization. In this paper the discrete wavelet transform is adopted in which the wavelets are orthogonal to each other.

The DWT in terms of  $\psi_{m,n}$  can be represented as

$$X_{m,n} = \sum_{k=1}^{n+1} x(k) \psi_{m,n}(k) \quad (1)$$

The signal  $x(t)$  can be represented by its DWT coefficients as:

$$x(t) = \sum_{n=-\infty}^{\infty} \sum_{m=-\infty}^{\infty} X_{m,n} \Psi_{m,n}(t) \quad (2)$$

Where,  $k$  = discrete variable,  $n, m$  = scaling variables,  $\psi$  = scaled and shifted versions of the wavelet function.

Wavelet transform uses short windows for high frequencies and long windows for low frequencies in contrast to STFT which uses a single analysis windows i.e. window length cannot be varied. Thus the frequency resolution is constant and depends on the width of the chosen window. But, frequency resolution can be varied for desired requirements in DWT as it has multiresolution capability which can be seen from the following theories.

### C. Multiresolution Wavelet Analysis (MRA)

The MRA is the new and powerful method of signal analysis well suited to fault generated signals. In MRA, the original signal is decomposed into 'scales' using wavelet prototype function called "mother wavelet" while frequency analysis is performed with a low frequency version of the mother wavelet and temporal analysis is performed with a high frequency version of the mother wavelet. Let  $x[n]$  be the discrete time signal,  $n$  is the samples. This signal is decomposed into  $c_1[n]$  and  $d_1[n]$  at scale 1, where  $c_1[n]$  is the smoothed version of the original signal and  $d_1[n]$  is the detailed version of the original signal. These are given by

$$c_1[n] = \sum_{k=1}^{n+1} h[k-2n] x[k] \quad (3)$$

$$d_1[n] = \sum_{k=1}^{n+1} g[k-2n] x[k] \quad (4)$$

Here  $h[n]$  and  $g[n]$  are the associated filter coefficients that decompose  $x[n]$  to  $c_1[n]$  and  $d_1[n]$  respectively. The next higher scale decomposition will be on  $c_1[n]$ . Thus at scale 2,  $c_1[n]$  is decomposed to  $c_2[n]$  and  $d_2[n]$  and so on. Thus the decomposition process can be iterated, with successive approximate being decomposed in turn, so that the original signal is broken down into much lower resolution compact,  $d_1[n]$  is used for threshold checking to estimate the change time-instants. The change time-instants can be estimated by the instants when the wavelet coefficients exceed a given threshold value. The detailed version only involves the fault identification and classification, which necessitate a smoothed version. The smoothed version is got by the following smoothing operations:

- It removes confusing multiple close-spikes and combines them into single unit impulse.
- It removes unwanted glitches, which can otherwise result in false positives for the abrupt changes.
- The segments in the power system fault analysis are during the pre-fault condition and the following

events like fault initiation, circuit-breaker opening and reclosing. These events are predefined and are the number of segments. So, any bigger number of segmentation possibly indicates transients, power swings and the like. Estimation of the number of segment(s) is also performed and checked to distinguish the fault from the transients, power swings, etc.

- (d) Based on the modeling of the segments, analysis is done for estimating the event-critical change instants, rejecting others.

Thus, MRA provides a more efficient way of representing a signal at different resolution scales.

### III. FAULT IDENTIFICATION AND CLASSIFICATION ON EHV LINES USING MRA METHOD

The fault is identified and classified using the faulted features extracted from the harmonics with the aid of MRA approach. The important parameter in the wavelet analysis is the wavelet type. After examination of several kinds of wavelet, the Daubechies-D4 wavelet [8, 11] is proved to have little computations burden and it is suitable for both low and high frequency analysis.

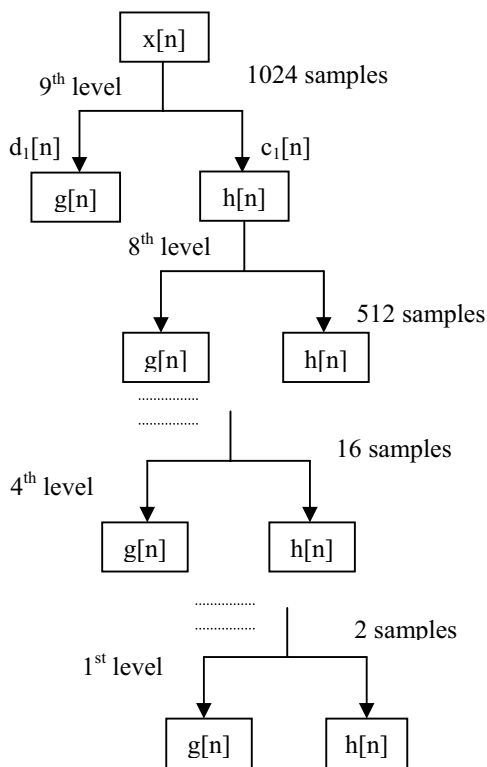


Fig. 3 Filter bank model implementation for MRA

#### A. Input Analysis

The current waveforms of the simulated power system using MATLAB packages are used to obtain the harmonic features of the faulted system. These current signals are to be fed to the sampling network where waveforms are sampled at 50 KHz

[5]. Then it necessitates sampling to view the fault features in elaborate manner.

#### B. Filter Bank Model

To extract the useful features the filter bank model shown in Fig. 3 are implemented. The data considered in the analysis is assumed to be of finite duration and of length  $2^N$ , where  $N=n+1$  is an integer. If  $N$  is chosen to be 10, the total duration of the analysis comes out to  $2^{10}$ . Sampling time considered in the analysis is  $20\mu s$ , which corresponds to the frequency of 50 KHz and the total number of samples considered is  $2^{10}=1024$ . Therefore, the duration required will be  $1024 \times 20\mu s = 0.2048ms$ . Various line lengths and various fault distances are taken into consideration to reveal that sampling frequency  $f_s$  and number of samples  $N$  are independent.

Thus the sampling will give higher resolution of the faulted signal as it involves 20 cycles of the 50Hz system. The discrete wavelet signal,  $x[n]$  with 1024 samples is passed through the high pass ( $g[n]$ ) and low passes ( $h[n]$ ) respectively. Further down sampling by 2, the next level (i.e., 9<sup>th</sup> level) DWT coefficients are obtained. Then, lower 512 samples are further passed through high pass and low pass filter respectively. This process continues till the 1<sup>st</sup> level DWT coefficients are obtained. In this work we tested the developed program with various mother wavelets through trial and error, that the D4 wavelet is suitable to discriminate all type of faults. Whereas other types of wavelets failed to differentiate a few. These values are suitable only for this power system under consideration. These values may have to be redefined for other power system based on trial and error, further a visual inspection on the detail plots found from MATLAB will serve as means to approximately determine these values. In this level 4(D4) and level 9(D9) are given to fault identification and classification algorithm.

#### C. PI Section (Lumped Parameter)

Generally in electromagnetic transient simulations, the most familiar method is to use Pi sections. A simple Pi section model will give the correct fundamental impedance. The transmission system is represented by lumped elements (usually by several cascaded pi sections) evaluated at a single frequency. A more sophisticated form of this type of model includes the representation of the ground return impedance using a suitable combination of several R-L branches. This representation is widely used in transient network analyzers. The validity of these models is restricted to relatively short lines or cables and, in general, their frequency response is only good in the neighborhood of the frequency at which the parameters are evaluated [16].

#### D. Fault Identification and Classification Algorithm

To begin with the fault identification and classification, the threshold values are to be selected to get the accurate result. The 4<sup>th</sup> level and 9<sup>th</sup> level are utilized to extract the sufficient features. This is because the 4<sup>th</sup> level details generally reflect the dominant transient signals generated by faults and the 9<sup>th</sup> level details contains most of the fundamental harmonic. The flowchart shown in Fig. 4 describes the procedure

involved in the fault identification and classification algorithm. The coefficients of 4<sup>th</sup> level detail( $y$ ) is adopted to identify the faults and if the three consecutive detail values are less than the threshold value ( $\tau_1$ ), then the fault can be claimed. Once the fault had occurred, determine  $X_p$  and  $y$  where,  $X_p$  is the maximum absolute value in each phase of 4<sup>th</sup> level detail and  $y = \max(x_a, x_b, x_c)$ . Then evaluate in which phase 'p' belongs to. The other parameters in the procedure are explained as follows,

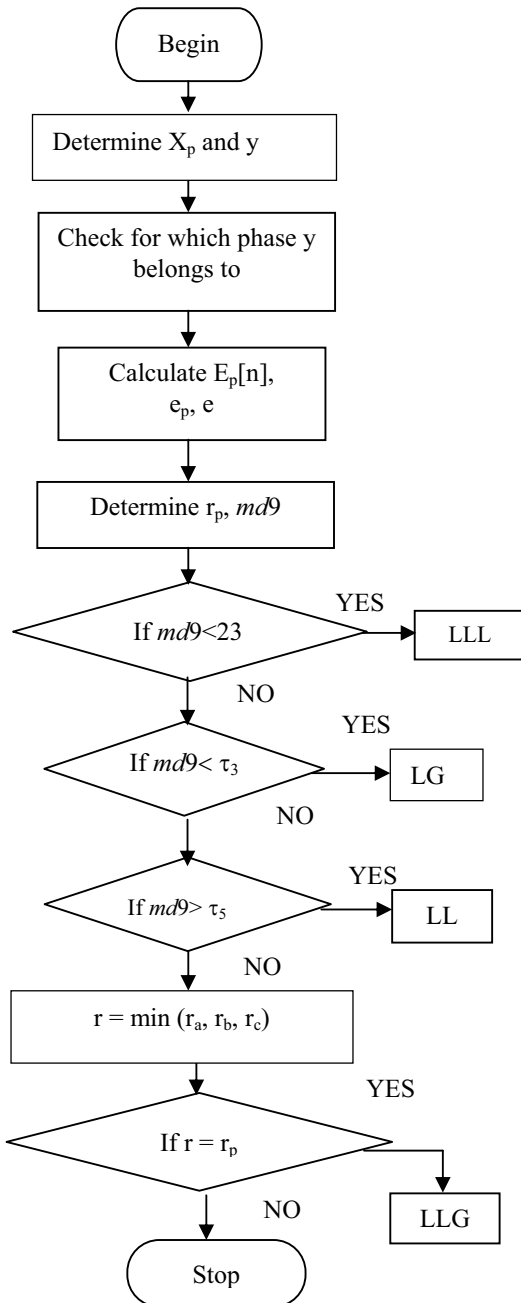


Fig. 4 Flow chart for the proposed Pi section method

$E_p[n']$  = maximum of the absolute values with respect to the three phases,  $n' = \{1, 2, 3\}$

$$e_p = E_p[1] + E_p[2] + E_p[3], p \in (a, b, c) \quad (5)$$

$$e = \max(e_a, e_b, e_c) \quad (6)$$

Where,  $e$  = Maximum value of  $e_p$

The ratio of  $e_p$  to  $e$  is defined as  $r_p$ . Then  $md9$  (maximum value of level 9 detail) is determined which is used for classification with respect to the threshold values.

If  $md9 < 23$ , then it is three phase fault. If  $md9 < \tau_3$ , then it is a LG fault and the discrimination among the phases involves another threshold value,  $\tau_4$ . If  $md9 > \tau_5$  and also if any two values among  $r_a, r_b, r_c$  are greater than  $\tau_4$ , then LL fault can be claimed. Then evaluate  $r$  which is defined as the minimum of  $r_a, r_b, r_c$ . If  $r$  is equal to any of these values, then LLG fault had occurred.

The threshold values ( $\tau_1, \tau_2, \tau_3, \tau_4$  and  $\tau_5$ ) are selected according to the detail, fault values in normal and fault operations on the transmission line.

Steps involved in fault identification and classification algorithm are as follows [1]:

1. Begin with variable initialization. Here variable refers to the fault current in transmission line.
2. Calculate level 4 details of three phases,  $D_{4p}$ . Where  $p \in (a, b, c)$ ,  $D_{4p}$  -- level 4 detail,  $p$  -- Phase, a, b, c -- a phase, b phase and c phase respectively. Detail -- high frequency correction, Level -- detail 4 is adopted because it gives us to analyze the fault in appropriate method.
3. For any one of the three phases, if the three consecutive absolute values of level 4 details are greater than threshold to be say  $\tau_1$ , then claim a fault. Otherwise move analysis window and go to step (1).
4. Calculate the max-absolute values of level 4 detail in each phase:  
 $X_p = \max(|D_{4p}(i)|), p \in \{a, b, c\}$ .  
Then obtain the maximum among three:  $y = \max(x_a, x_b, x_c)$ .
5. Check to which phase  $x$  belong to. If  $y = X_p$ , let  $k = i_p$ ,  $X_p$  --  $x$  belongs to phase ( $p \in a, b, c$ ),  $i_p$  - index of  $X_p$ ,  $k$  -  $k$  th value index used in result analysis.
6. Let  $E_p(n') = |D_{4p}(k+n'-1)|, p \in \{a, b, c\}, n' = 1, 2, 3$ .
7. Calculate  $e_p = \sum E_p(n')$ ,  $p \in (a, b, c)$ , where  $e_p$  -- summation of  $E_p(1), E_p(2), E_p(3)$
8. Calculate  $e = \max(e_a, e_b, e_c)$
9. Calculate ratio of each phase:  $r_p = e_p/e, p \in a, b, c$
10. Calculate the sum of three phase level 9 details as same procedure as of detail-4.  
 $D_9 = D_{9a} + D_{9b} + D_{9c}, md9 = \max(|D_9(i)|)$   
It is done up to level - 9 detail, to get accurate information for fault classification in result.
11. If  $md9 < 23$ , it's a three-phase fault.
12. If  $|r_a - r_b| - |r_b - r_c| > \tau_2, |r_a - r_c| - |r_b - r_c| > \tau_2, md9 < \tau_3$ , it's A-G fault.
13. If  $|r_b - r_c| - |r_a - r_c| > \tau_2, |r_b - r_a| - |r_a - r_c| > \tau_2, md9 < \tau_3$ , it's B-G fault.
14. If  $|r_c - r_a| - |r_b - r_a| > \tau_2, |r_c - r_b| - |r_b - r_a| > \tau_2, md9 < \tau_3$ , it's C-G fault.
15. If  $r_a > \tau_4, r_b > \tau_4, md9 > \tau_5$ , it's A-B fault.

16. If  $r_c > \tau_4$ ,  $r_b > \tau_4$ , and  $md9 > \tau_5$ , it's C-B fault.
17. If  $r_a > \tau_4$ ,  $r_c > \tau_4$ , and  $md9 > \tau_5$ , it's A-C fault.
18. Let  $r = \min(r_a, r_b, r_c)$
19. Let  $r = r_a$ , it is a BC- G fault.
20. Let  $r = r_b$ , it is a AC- G fault.
21. Let  $r = r_c$ , it is a AB- G fault.
22. End.

#### IV. FAULT IDENTIFICATION AND CLASSIFICATION ON EHV LINES USING ANN METHOD

##### A. Neural Fault Detector

The fault detection task can be formulated as a pattern classification problem. The fully connected three-layer feed forward neural network is used to classify faulty/non-faulty data sets and the back-propagation algorithm is used for training. The numbers of neurons in the input and hidden layers were selected empirically through extensive simulations. Various network configurations are trained and tested in order to establish an appropriate network with satisfactory performances, which are the fault tolerance, time response and generalization capabilities. With supervised learning, the Artificial Neural Network (ANN) is trained with various input patterns corresponding to different types of fault (a-g, b-g, c-g, a-b-g, a-c-g, b-c-g, a-b, a-c, b-c, a-b-c and a-b-c-g, where a, b, and c are related to the phases and g refers to the ground) at various locations. In order to build up an ANN, the inputs and outputs of the neural network have to be defined for pattern recognition. The input to the network should provide a true representation of the situation under consideration. The process of generating input patterns to the ANN Fault Detector (FD) is depicted in Fig. 5.

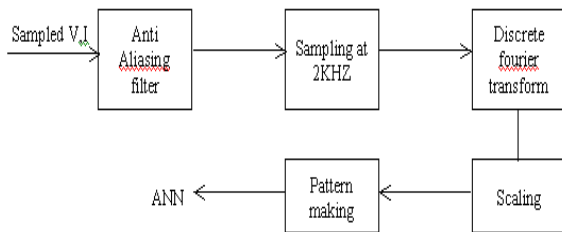


Fig. 5 Processor for generating input patterns to the ANN fault detector

##### B. Discrete Fourier Transform with ANN Results [15]

The method for classifying faults using DFT is analyzed in the following aspects. To perform frequency analysis, the signal to be converted from the time-domain signal to frequency domain and the frequency analysis to be performed requires infinite number of samples which does not provided by z-transform. So, DFT is used to perform the frequency analysis of the sampled signals as it provides number of samples. In this method FFT (Fast Fourier Transform) is used to find the three phase signals. The current (I) and voltage (V) signals are calculated as a string of samples corresponding to a 2 kHz sampling frequency (40 samples per 50 Hz cycle) using an anti-aliasing filter to remove the unwanted

frequencies from a sampled waveform. This sampling rate is compatible with sampling rates presently used in digital relays. The phase current ( $I_a, I_b, I_c$ ) and voltage ( $V_a, V_b, V_c$ ) signals, and the zero sequence current ( $I_0$ ) and voltage ( $V_0$ ) signals sampled at 2 kHz are used as the inputs to the ANN. The voltage and current signals are fed to DFT filters for extraction of the fundamental phasor magnitudes [3]. One full cycle DFT filter is utilized to obtain the magnitudes of the signals just after the fault occurrence and only the fundamental frequency component is used. It should be mentioned that the input current and voltage samples have to be normalized in order to reach the ANN input level ( $\pm 1$ ). The ANN output is indexed with the value either 1 (the presence of a fault) or 0 (the non-faulty situation) and from that classifies the fault.

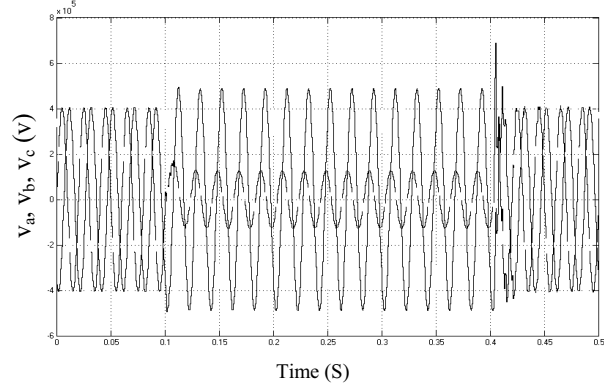


Fig. 6 Voltage waveform for single phase to ground fault (a-g) with  $R_f=5\Omega$  and  $R_g=10\Omega$  corresponds to the fault transition times 0.1s, 0.4s.

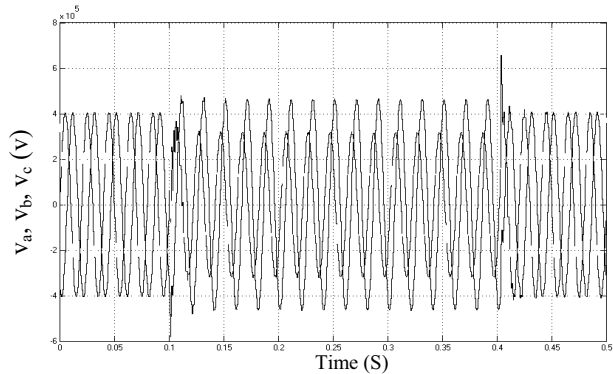


Fig. 7 Voltage waveform for double phase to ground fault (a-b-g) with  $R_f=40\Omega$  and  $R_g=10\Omega$  corresponds to the fault transition times 0.1s, 0.4s

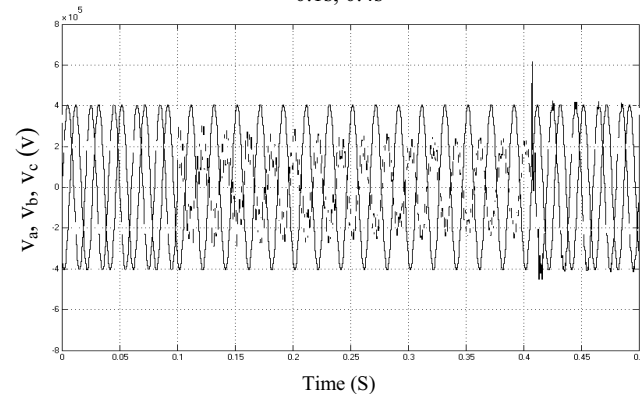


Fig. 8 Voltage waveform for line to line fault (a-b) with  $R_f=0.001\Omega$  and  $R_g=10\Omega$  corresponds to the fault transition times 0.1s, 0.4s

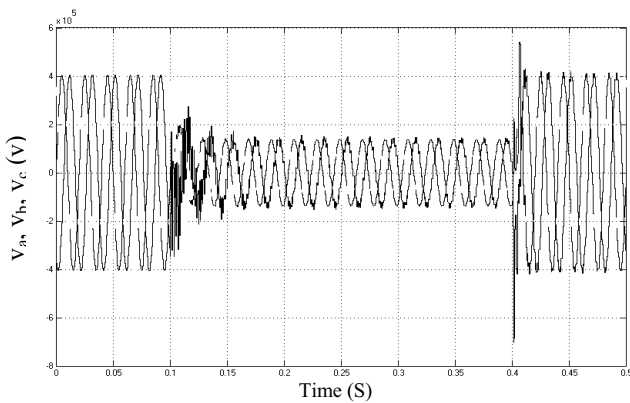


Fig. 9 Voltage waveform for three phase fault (a-b-c) with  $R_f=10\Omega$  and  $R_g=10\Omega$  corresponds to the fault transition times 0.1s, 0.4s.

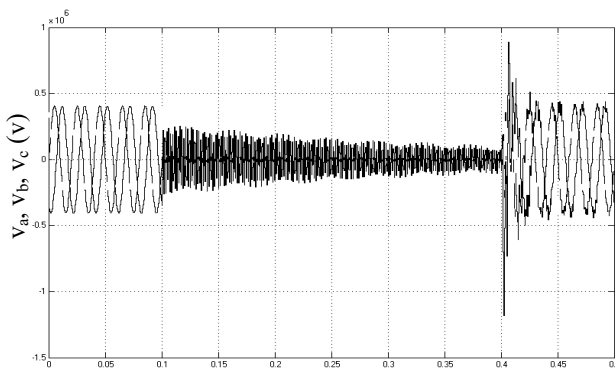


Fig. 10 Voltage waveform for three phase to ground fault (a-b-c-g) with  $R_f=0.001\Omega$  and  $R_g=10\Omega$  corresponds to the fault transition times 0.1s, 0.4s.

The performance characteristics of the ANN fault detector are [5, 15]:

(a) The minimal response time  $t_r$  of fault detection is the difference between the desired fault detection time value  $t_d$  and the actual fault detection time value  $t_a$ :

$$t_r = t_a - t_d \quad (7)$$

(b) Generalization capabilities are: A good ANN fault detector is obtained when the response time is minimal, the ANN output values are stable in both the normal (e.g., 0) and fault (e.g., 1) conditions, and capable of providing fast and accurate fault detection in a various fault situations.

(c) The only means of verifying the performance of a trained neural network is to perform extensive testing. After training, the neural fault detector is then extensively tested using independent data sets consisting of different fault scenarios that were never used previously in training. As mentioned before, the fault detector performances are evaluated in terms of the  $t_r$  of the fault and the best performances are obtained when  $t_r$  is minimal. The neural fault detector was tested with 90 new fault conditions for each type of fault [3]. After the training, the neural fault detector was tested with 5 new fault conditions and different power system data with learning rate  $\eta = 0.05$  sampling time  $T_s = 0.0005\text{Sec}$ . Fig. 6 to Fig. 10 shows the phase and zero sequence voltage waveforms.

Fig. 6 illustrate the voltage waveform of a-g fault with the transition times 0.1Sec, 0.4Sec with time in X axis and three

voltages ( $V_a, V_b, V_c$ ) in Y axis. In this waveform, a fault occurs in phase 'a', so 'a' phase voltage alone is reduced from its normal value while other two phases 'b' and 'c' are increased with their voltage, where  $R_f$  = fault resistance,  $R_g$  = ground resistance. Similarly Fig. 7 illustrate the voltage waveform of a-b-g fault, in this a and b phase voltages gets reduced and c phase is increased.

Fig. 8 illustrate the voltage waveform of a-b fault, here the a and b phase voltage is reduced and there is a slight variation in c phase. Then in Fig. 9 all the three phase voltages are dropped from their original value. Similarly in Fig. 10, the voltages of the all phases are further dropped compared to Fig. 9. The results reveal that the neural network is able to generalize the situation from the provided patterns [15]. It indicates the presence or the absence of a fault and can be used for on-line fault detection. It can be seen that the maximum  $t_r$  is 1 ms. A number of 99.54% of fault cases are detected within a time of 0.5 ms and a number of 0.45% of the tested cases are detected within a time of 1 ms. All faults are detected within a time of less than 1 ms, which indicates its usage for on-line fault detection [15].

## V. RESULTS AND DISCUSSIONS

### A. Wavelet Results

The simulations were done on a simple transmission line circuit consisting of a generator at one end and a load at the other end and the line is extended to 150 km. The base value of the voltage in the system is 400kV. When the proposed method is used, the desired data window length must be adopted. Two important aspects must be considered: the window contains enough information to obtain the required wavelet levels and it is short enough to produce the expected speed. Hence, fault identification and classification is done with the aid of some ratios  $r_p$ , where p stands for phase a, b and c and  $md9$  is the maximum value of 9<sup>th</sup> level detail. Fig. 11 to Fig. 14 are results of Pi section and ' $\tau$ ' is the threshold value. For any type of fault, the ratio  $r_p$  and  $md9$  should have a particular value.

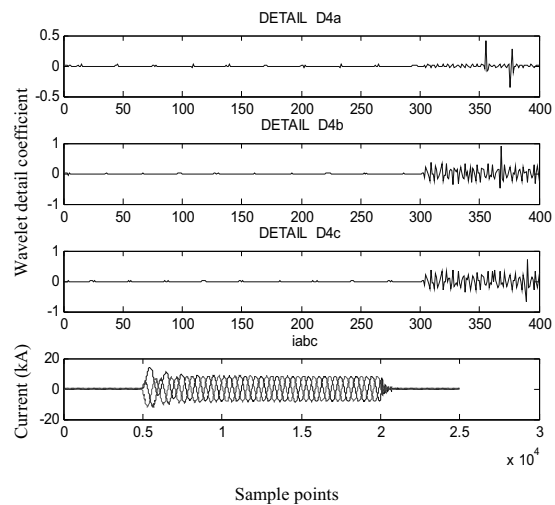


Fig. 11(a) Wavelet analysis for a-b-c fault

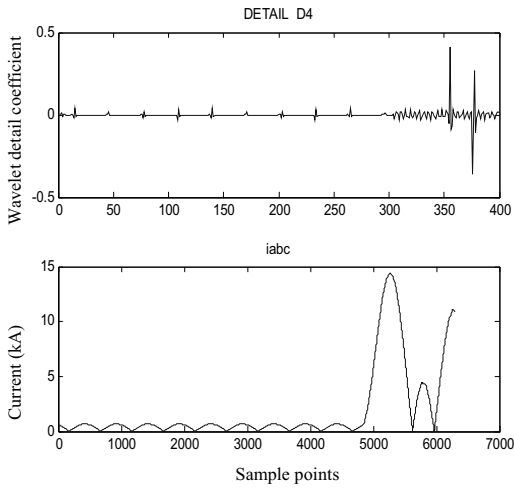


Fig. 11(b) Wavelet transient form of a-b-c fault

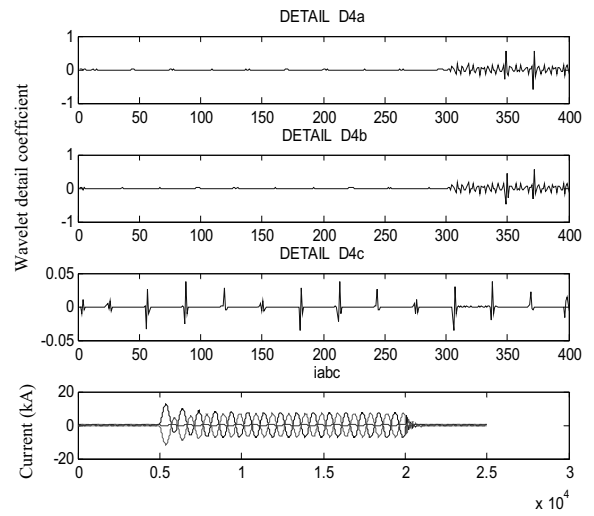


Fig. 13(a) Wavelet analysis for a-b fault

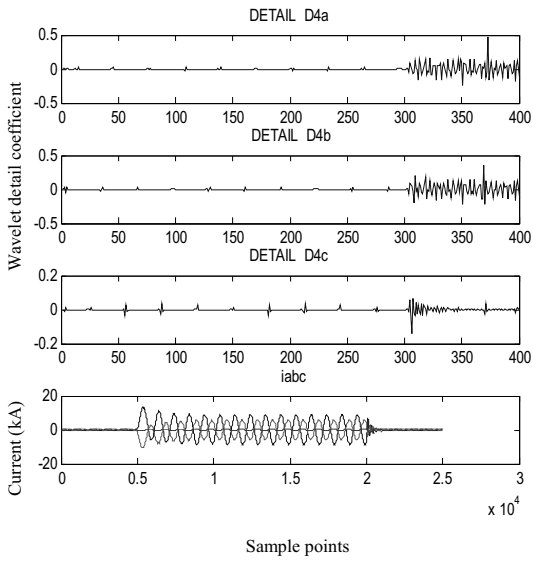


Fig. 12(a) Wavelet analysis for a-b-g fault

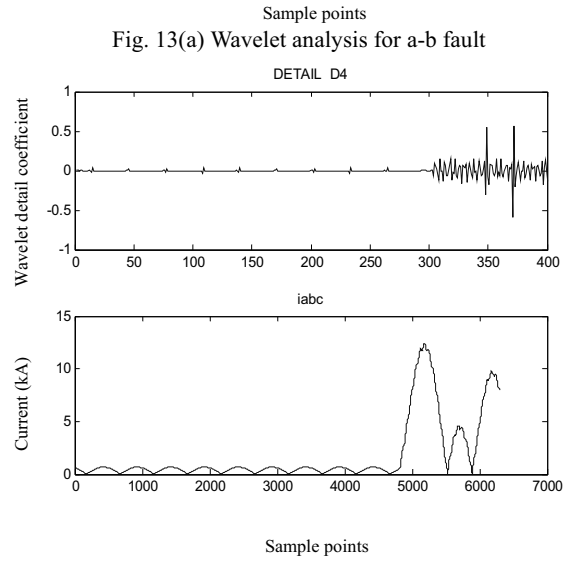


Fig. 13(b) Wavelet transient form of a-b fault

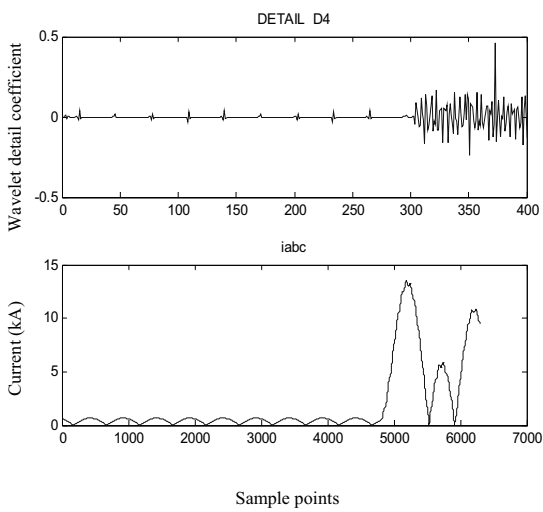


Fig. 12(b) Wavelet transient form of a-b-g fault

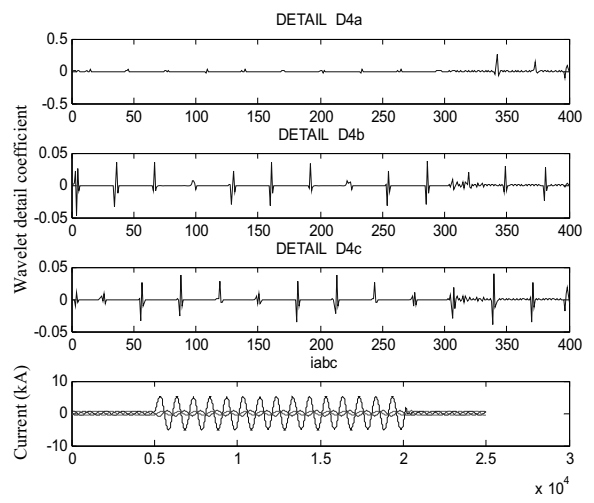


Fig. 14(a) Wavelet analysis for a-g fault

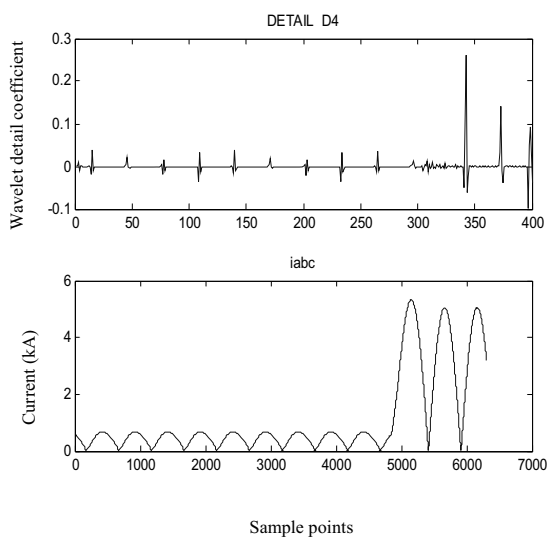


Fig. 14(b) Wavelet transient form of a-g fault

Based on 50 KHz sampling rate, fault classification is performed using the features extracted from level 4 detail wavelet analysis as level 4 detail (D4) is the best when compared to other details, so D4 is taken to fix the threshold values by finding minimum and maximum wavelet coefficient values of D4 detail. From the analysis the threshold values of  $\tau_1, \tau_2, \tau_3, \tau_4$  and  $\tau_5$  are fixed, Fig. 11 (a) shows the signal feature extracted from the a-b-c fault with separately indicating the detailed current waveform of phase a,b,c as the details D4a, D4b, D4c respectively. The waveform iabc is the original current waveform of the fault signal of phases a, b and c.

Then in Fig. 11(b), Detail D4 is the combined faulted wavelet transient waveform of phases a, b and c and iabc is the wavelet transient waveform of combined original fault signal with phases a, b and c. similarly Fig. 12 illustrate the waveforms of a-b-g fault, Fig. 13 shows the a-b fault waveforms and Fig. 14 illustrate the waveforms of a-g fault. The threshold values are very much important to find the type of fault, as these threshold values decide what type of fault has occurred in the transmission line.

### B. Comparative Table of Discrete Wavelet Transforms

The fault classification algorithm of underground cable [1] also involves the threshold values, but the discrimination among different phases is not efficient. To overcome this, five threshold values are selected accordingly. From the current waveform 9 level details are obtained using wavelet transform. Here all types of faults are considered, fault classification is performed using the features extracted from level 4 detail wavelet analysis as level 4 detail is the best when compared to other details, so D4 is taken to fix the threshold values by finding minimum and maximum wavelet coefficient values of D4 detail.

From the analysis  $\tau_1, \tau_2, \tau_3, \tau_4$  and  $\tau_5$  values are fixed. Here the threshold values are  $\tau_1 = 0.45, \tau_2 = 0.7, \tau_3 = 50, \tau_4 = 0.3, \tau_5 = 90$ .

The waveforms that are obtained as the result are shown in Fig. 11 to Fig. 14, in which the x-axis represents sample

points and y axis represents the wavelet coefficient of 4<sup>th</sup> level detail.

TABLE I  
RESULTS OF LLL FAULT FOR THE PROPOSED METHOD

LLL FAULT	Pi Section
k	390
y	0.7233
md9	22.42
r	0.025268
r <sub>p</sub>	
r <sub>a</sub>	0.025268
r <sub>b</sub>	1
r <sub>c</sub>	0.26081

TABLE II  
RESULTS OF LLG FAULT FOR THE PROPOSED METHOD

LLG FAULT	Pi Section		
	a-b	b-c	c-a
k	307	364	317
y	0.0657	0.9251	0.4365
md9	153.7636	96.4423	91.7735
r	0.013887	0.0055877	0.07558
r <sub>p</sub>			
r <sub>a</sub>	1	0.0055877	0.32666
r <sub>b</sub>	0.22244	0.26775	0.07558
r <sub>c</sub>	0.013887	1	1

TABLE III  
RESULTS OF LL FAULT FOR THE PROPOSED METHOD

LL FAULT	Pi Section		
	a-b	b-c	c-a
k	338	333	359
y	0.0381	0.7353	0.3010
md9	151.55	96.369	93.082
r <sub>p</sub>			
r <sub>a</sub>	1	7.3718e-006	1
r <sub>b</sub>	0.96885	1	1.6685e-005
r <sub>c</sub>	1.3662e-005	0.73512	0.34046

TABLE IV  
RESULTS OF LG FAULT FOR THE PROPOSED METHOD

LG FAULT	Pi Section		
	a-b	b-c	c-a
k	340	307	384
y	0.0394	0.1143	0.2073
md9	41.387	39.653	24.515
r <sub>p</sub>			
r <sub>a</sub>	1	0.036166	0.02521
r <sub>b</sub>	0.005805	1	0.025209
r <sub>c</sub>	0.0088531	0.036109	1

From the Table I, the valuable information to classify the fault is obtained. According to the flow chart shown in Fig. 4, the value of md9<23, then it is a LLL fault. From the Table I



the md9 value for a-b-c fault is 22.42 which is less than  $\tau_3 = 23$ , so it is claimed to be a-b-c fault. Fig. 11 shows the details of LLL fault (a-b-c result). Fig. 11(a) shows the fault in each phase separately. The result can be obtained in transient form by adding up all the individual phase faults as shown in Fig. 11(b), with the values given in Table I, from the above details it is found to be LLL (a-b-c) fault.

To claim the fault as LL fault, the md9 value for a-b fault is 151.55 which are shown in Table III. From the flowchart in Fig. 4, if the value of  $md9 > \tau_5 = 90$ , then it is placed as LL fault, as 151.55 is greater than 90 where, y is the actual maximum value of coefficient details, k is index of y, rp is the ratio with respect to phases. Similarly Fig. 13 shows the details of LL fault (a-b fault) Fig. 13(a) represents the fault in each phase separately. It is found that in a-b-g fault, there is a fault in a and b phase. Fig. 13(b) shows the adding up of a, b and c phase faults and representing it in transient form. With the values given in Table III it is found to be LL (a-b) fault. Similarly Fig. 12 shows LLG fault, if any one of the  $r_a, r_b, r_c$  value is equal to r value then it is LLG fault, details are shown in Table II and Fig. 14, shows LG fault, all the md9 values are less than  $\tau_3 = 50$  value, details are shown in Table IV.

Generally in electromagnetic transient simulations most familiar method is to use Pi sections. A simple Pi section model will give the correct fundamental impedance. Pi section is suitable for very short lines where the traveling wave models cannot be used. The validity of Pi section model is restricted to relatively short lines or cables and, in general, their frequency response is only good in the neighborhood of the frequency at which the parameters are evaluated. The proposed approach validity is proved to be effective and accurate in Pi section models.

## VI. COMPARISON OF RESULTS OBTAINED

From the analysis of the graph of DFT based ANN, it can be understood that, due to fluctuation, some of the phase undergoes disturbance without occurring fault. This small disturbance may change the value in minute order. Even this minute change may give classification from one form to another. For example, based on the value, it may be LL fault but due to fluctuation there may be minute change in the value and DWT will give the accurate result as LLG fault and not as LL fault. This accuracy is attained by using this proposed approach based on the values. Compare to DFT based ANN, DWT is the best method for classification of fault because,

- (a) Finding sampling data is easier due to MRA method.
- (b) DFT based ANN are trained with various set of input pattern and for each set there is a separate set of waveforms where as in DWT analysis only one training pattern is enough for all data.
- (c) DWT takes less time duration for simulation and also for execution (DFT based ANN 0.0005 Sec, DWT 2e-005 Sec).
- (d) In case of DFT based ANN if there is a fault in the particular line, then that particular line alone be considered for fault classification, while in DWT analysis

all the three phases will be considered for fault classification, hence DWT analysis is the very effective one to detect the accurate fault type.

- (e) It is not possible to correctly distinguish between LL and LLG faults using DFT based ANN as the ratios overlap for most of the cases, but it is very much possible in DWT, hence DWT has better accuracy in fault detection.

## VII. CONCLUSION

In this paper, the MRA wavelet transform is implemented and proved to be accurate and efficient when compared to the approach implemented earlier [5,15] for the classification of faults. The results are obtained in very short duration of time. The discrimination in the fault classification of the proposed method is accurate as it includes the threshold values and the variations in the other phases. Here level 4 and level 9 details are utilized to extract some useful features. Level 4 dominant transient signals are generated by faults and level 9 details contain most of the fundamental harmonics. The localization of time in the wavelet transform is the most advantageous one in contrast to other transforms. Compared to DFT based ANN, DWT is the efficient method for classification of fault because DWT gives better accuracy in fault detection where time and frequency are considered, thus easy to identify the fault and finding sampling data is also easier. Less time duration for simulation and also for execution (DFT based ANN 0.0005 Sec, DWT 2e-005 Sec) is achieved in the proposed method. It is not possible to correctly distinguish between LL and LLG faults using DFT based ANN as the ratios overlap for most of the cases, but it is very much possible in DWT. These indicate the potentials of wavelet in detecting the fault transient signals in the power system, discriminating from other signals and classifying the faults on the EHV transmission line. The proposed method is also applicable to a double-circuit untransposed line as a future work.

## REFERENCES

- [1] W. Zhao, Y.H. Song and Y. Min, "Wavelet analysis based scheme for fault detection and classification in underground cable system," *Electric Power Systems Research*, vol. 53, pp. 23-30, 2000.
- [2] Z.Q. Bo, R.K. Aggarwal A.T. Johns, H.Y. Li and Y.H. Song, "A new approach to phase selection using fault generated frequency noise and neural networks," *IEEE Trans. Power Delivery*, Vol. 12, no.1, pp 106-113, 1997.
- [3] Z.Q. Bo, R.K. Aggarwal A.T. Johns, H.Y. Li and Y.H. Song, "A new approach to phase selection using fault generated frequency noise and neural networks," *IEEE Trans. Power Delivery*, Vol. 12, no.1, pp 106-113, 1997.
- [4] M. Oleskovicz, D.V. Coury and R.K. Aggarwal, "A complete scheme for fault detection, classification and localization in transmission lines using neural network," *Proc. 7-th Int. Conf. Developments in Power System Protection*, Amsterdam, the Netherlands, pp. 335-338, 2001.
- [5] D. Das, N.K. Singh and A.K. Singh, "A Comparison of Fourier transform and Wavelet Transform Methods for Detection and Classification of faults on Transmission Lines," *Proc. 2006 IEEE Power India conf.*, New Delhi, India, Ab. Sl. No. 237, April 2006.
- [6] S. P. Bingulac, "On the compatibility of adaptive controllers (Published Conference Proceedings style)," in *Proc. 4th Annu. Allerton Conf. Circuits and Systems Theory*, New York, 1994, pp. 8-16.
- [7] J.R. Partington, "On the windowed Fourier Transform and Wavelet Transform of Almost Periodic Functions," *Applied and Computational Harmonic Analysis*, vol. 10, pp. 45-60, 2001.

- [8] I.K. Yu and Y.H. Song, "Development of novel adaptive single-pole autoreclosure scheme for extra high voltage transmission systems using wavelet transform analysis," *Electric Power Systems Research*, vol. 47, pp. 11-19, 1998.
- [9] Abhisek Ukil and Rastko Zivanovic, "Abrupt change detection in power system analysis using adaptive whitening filter and wavelet transform," *Electric Power Systems Research*, vol. 76, pp. 815-823, 2006.
- [10] Dong Xinzhou, Genge Zhong Xing, Ge Yaozhong and Zhong Fusheng Xu Bingyin, "Application of Wavelet Transform on Power System Fault Analysis," *Chinese Soc. of Electrical Engg.*, vol. 7, no. 6, pp. 421-424, 1997.
- [11] J. Liang, S. Elangovan and J.B.X. Devotta, "A wavelet multiresolution analysis approach to fault detection and classification in transmission lines," *Electrical Power and Energy Systems*, vol. 20, no. 5, pp. 327-332, 1998.
- [12] D. Chanda, N.K. Kishore and A.K. Sinha, "Application of wavelet multiresolution analysis for identification and classification of faults on transmission lines," *Electric Power Systems Research*, vol. 73, pp. 323-333, 2005.
- [13] Ronald R. Coifman and Mauro Maggioni, "Diffusion wavelets," *Applied and Computational Harmonic Analysis*, vol. 21, pp. 3-94, 2006.
- [14] Julio Barros and Ramon I. Diego, "A new method for harmonic groups in power systems using wavelet analysis in the IEC standard framework," *Electric Power Systems Research*, vol. 76, pp. 200-208, 2006.
- [15] K. Gayathri and N. Kumarappan, "ANN Based Fault Detection and Location in EHV Transmission Lines," *Proc. 38-th North American Power Symposium*, Carbondale, Illinois (US), pp. 559-565, September 2006.
- [16] L.Marti, "Simulationn of Transients in Underground Cables with Frequency-Dependent Model Transformation Matrices," *IEEE Trans. Power Delivery*, Vol. 3, no.3, pp 1099-1110, 1988.
- [17] K. Gayathri, N. Kumarappan and S.Guruprasad, "EHV Transmission Line Modeling Using PS-CAD Based on EMTDC Technique," Bangalore, pp. , December 2007.



**K.Gayathri** was born on April 10, 1976. She completed her B.E. degree in Electrical and Electronics in 1999 and M.E. degree in Power Systems in 2005 at Annamalai University. She is presently a Senior Lecturer and also doing her PhD degree at Annamalai University, India. Her research interests include power system analysis, fault Diagnosis and artificial intelligence techniques to power systems.



**N.Kumarappan** was born on November 27, 1961. He was graduated from Madurai Kamaraj University in 1982; post graduated from Annamalai University in 1989 and received his PhD at CEG Anna University in 2004, India. He is presently a Professor in the Annamalai University. His research interests include power system operation and control; power system reliability and artificial intelligence techniques. He is the life fellow of Institution of Engineer's (India) and life member of Indian society of Technical Education. He is the senior member of the IEEE (USA).